

# Contamination and Space Environmental Effects on Solar Cells and Thermal Control Surfaces

Joyce A. Dever\*

NASA Lewis Research Center, Cleveland, Ohio 44135

Eric J. Bruckner†

Cleveland State University, Cleveland, Ohio 44115

and

David A. Scheiman‡ and Curtis R. Stidham‡

NYMA, Inc., Brook Park, Ohio 44142

For surfaces in low Earth orbit on the International Space Station, contamination may occur from Space Shuttle thruster exhaust, sputter contamination products, and products of silicone degradation. Interaction of the natural low-Earth-orbit environment with the surface contaminants may degrade the performance of solar cells and thermal control coatings. This paper describes laboratory testing in which solar-cell materials and thermal control surfaces were exposed to simulated space environmental effects including contamination, atomic oxygen, ultraviolet radiation, and thermal cycling. Contamination from thruster exhaust in amounts significantly exceeding those expected on the Space Station resulted in increased solar absorptance of surfaces and in degradation of solar-cell performance. Fused silica samples that were subsequently exposed to an environment dominated by atomic oxygen and containing some vacuum-ultraviolet radiation showed reversal of this degradation. Materials which were exposed to vacuum-ultraviolet radiation subsequent to thruster-exhaust contamination showed slight additional degradation in solar absorptance. Despite significant differences between the simulated environments and the low-Earth-orbit environment, these data are useful in suggesting possible trends in performance changes for solar cells and thermal control surfaces due to the interactions between surface contaminants and the natural low-Earth-orbit environment.

## Nomenclature

$E(\lambda)$	= spectral irradiance of the sun, $\text{W/m}^2 \cdot \text{nm}$
$\alpha_s$	= solar absorptance
$\epsilon_n$	= total normal emittance
$\lambda$	= wavelength, nm
$\rho(\lambda)$	= spectral reflectance
$\rho_s$	= solar reflectance
$\tau(\lambda)$	= spectral transmittance
$\tau_s$	= solar transmittance

## Introduction

IN order to predict the long-term performance of solar cells and passive thermal control surfaces on low Earth orbit (LEO) missions such as the Space Station, it is necessary to know how optical properties of such materials will change owing to contamination in the presence of the natural LEO environment. Sources of contamination for Space Station surfaces include Space Shuttle thruster exhaust, products of sputtering from negatively biased surfaces, and products of degradation of silicones. Products of incomplete combustion of Space Shuttle thruster fuel are condensable and could contaminate nearby surfaces impinged upon by the thruster plume.<sup>1–6</sup> On the Space Station, surfaces that are at a negative potential relative to the plasma environment of space

will attract positively charged ionized gases, resulting in sputtering of those surfaces if the potential differences are sufficiently high.<sup>7</sup> Products of this sputtering can deposit onto nearby surfaces. It is possible that the anodized aluminum truss of Space Station will undergo sputtering, resulting in aluminum deposition onto the solar arrays, which then oxidizes to form aluminum oxide. Silicones used on spacecraft include adhesives for solar cells, potting compounds, wiring insulation, and coatings for solar array blankets. Outgassing products of silicones in LEO may cause contamination of nearby surfaces.<sup>8–11</sup> Even for silicone materials that have passed outgassing requirements for a LEO mission, such outgassing products may be released upon atomic-oxygen attack of the silicone surface. This paper describes laboratory testing to determine trends in the combined effects of the natural LEO environmental constituents such as atomic oxygen, ultraviolet radiation, and temperature cycling with contaminated solar-cell and thermal control surfaces. Because of the complexities associated with simulating the natural LEO and contamination environments, these experiments have obvious deficiencies compared to actual flight experiments. Furthermore, some flight experiments have been performed to address these issues.<sup>6</sup> However, because flight experiments are typically quite short in duration and are very expensive, ground laboratory testing such as this can be very useful in determining trends in long-term on-orbit performance of materials.

## Experimental

### Materials Evaluated

Three sample trays were prepared for exposure to thruster exhaust contamination. Table 1 describes the contents of these trays. They are shown in Fig. 1. Samples included 2.5-cm-diam fused silica disks, five of which were contaminated with  $1200 \pm 120 \text{ \AA}$  of dimethylsiloxane fluid prior to thruster exposure. Z-93-P, a white thermal control paint consisting of zinc oxide pigment in a potassium silicate binder, was applied to 2.5-cm-diam substrates of aluminum alloy 6061-T6. Also included were one sample of each of the following types of anodized aluminum materials: chromic-acid-anodized aluminum alloy 2219-T851, sulfuric-acid-anodized aluminum alloy

Received June 2, 1994; presented as Paper 94-2627 at the AIAA 18th Aerospace Ground Testing Conference, Colorado Springs, CO, June 20–23, 1994; revision received March 14, 1995; accepted for publication March 14, 1995. Copyright © 1995 by the American Institute of Aeronautics and Astronautics, Inc. No copyright is asserted in the United States under Title 17, U.S. Code. The U.S. Government has a royalty-free license to exercise all rights under the copyright claimed herein for Governmental purposes. All other rights are reserved by the copyright owner.

\*Materials Engineer, Electro-Physics Branch, Power Technology Division, 21000 Brookpark Road, MS 309-2, Member AIAA.

†Research Associate, Department of Physics.

‡Research Engineer, Aerospace Technology Department, 2001 Aerospace Parkway.

**Table 1** Contents of sample trays for thruster exposure

Tray no.	Samples	Qty.
1	Fused silica	12
	Silicone-contaminated fused silica	4
	Stainless steel	3
2	Fused silica	3
	Silicone-contaminated fused silica	1
	Z-93-P on aluminum	6
	Anodized aluminum	3
	Stainless steel	3
3	Al <sub>2</sub> O <sub>3</sub> -contaminated solar cells	2
	Stainless steel	2

2219-T851, and high-emittance Duranodic™ black (HEDB) anodize on alclad aluminum alloy 7075-T6. These samples were 2.5 by 2.5 cm.

Two 8 by 8 cm solar cells with cover glass of the type to be used on the Space Station were coated with  $835 \pm 68 \text{ \AA}$  of aluminum oxide (Al<sub>2</sub>O<sub>3</sub>) using electron-beam evaporation to simulate contamination from sputter deposition prior to installation on tray 3 for additional contamination from thruster exhaust. Stainless-steel witness coupons of 2.5-cm diam were also included on each tray.

### Sample Characterization

Spectral transmittance and reflectance between 250 and 2500 nm were obtained using an ultraviolet-visible-near-infrared (UV-VIS-NIR) spectrophotometer equipped with a 60-mm-diam integrating sphere. These data were used to calculate the solar absorptance of samples. The solar transmittance and solar reflectance values can be represented by

$$\tau_s = \frac{\int_{250 \text{ nm}}^{2500 \text{ nm}} \tau(\lambda) E(\lambda) d\lambda}{\int_{250 \text{ nm}}^{2500 \text{ nm}} E(\lambda) d\lambda} \quad (1)$$

$$\rho_s = \frac{\int_{250 \text{ nm}}^{2500 \text{ nm}} \rho(\lambda) E(\lambda) d\lambda}{\int_{250 \text{ nm}}^{2500 \text{ nm}} E(\lambda) d\lambda} \quad (2)$$

The solar absorptance was calculated for transparent samples by

$$\alpha_s = 1 - (\tau_s + \rho_s) \quad (3)$$

and for opaque samples by

$$\alpha_s = 1 - \rho_s \quad (4)$$

The accuracy in the measurement of  $\alpha_s$  is expected to be approximately  $\pm 0.02$ . This significant error is attributed to the small size of the integrating sphere. The repeatability is expected to be approximately  $\pm 0.005$ .

For opaque samples, the room-temperature total normal emittance  $\epsilon_n$  between 5 and 25  $\mu\text{m}$  was measured with an infrared reflectometer. The repeatability in measurements is expected to be  $\pm 0.005$ . A high-emittance and a low-emittance standard were used to calibrate the instrument prior to each measurement.

Stainless-steel witness coupons were weighed before and after thruster exposure to determine the mass of deposited contaminants. In order to identify the composition of the deposited contaminants, one of these witness coupons was studied with micro-Fourier-transformed infrared ( $\mu$ -FTIR) spectroscopy. The analysis was done using a  $15 \times$  Cassegranian objective over an area 100  $\mu\text{m}$  in diameter at the center of the sample.

The solar-cell air mass zero (AM0) efficiency was obtained by measuring current-voltage ( $I$ - $V$ ) characteristics while the cell was under illumination. These measurements were made using separate current and voltage leads (four-wire), measurement obtaining voltage directly off the cell and current across a shunt resistor. The cell was biased at various voltages using a dc power supply. Illumination was provided by a xenon-arc solar simulator with filtering to approximate the AM0 solar spectrum. A monitor solar cell was used to correct the cell current for variations in light intensity, which are up to 1–2%. The efficiency was calculated using an AM0 standard of 136.7 mW/cm<sup>2</sup>.

### Exposure to Thruster Exhaust

The three sample trays were exposed in the Space Shuttle Primary Reaction Control System (PRCS) thruster facility (test cell 405) at NASA White Sands Test Facility in White Sands, New Mexico. The PRCS bipropellant thruster uses monomethylhydrazine (MMH) fuel and a nitrogen tetroxide (N<sub>2</sub>O<sub>4</sub>) oxidizer. Samples were exposed in the test cell at a region near the outer edge of the exhaust plume, for up to three increments of 30.6 s of thruster-on time, during pulsed firing operation. Figure 2 shows the configuration of the sample trays with respect to the thruster. Figure 2a is a photograph of the three sample trays in the thruster facility. As can be seen in Fig. 2b

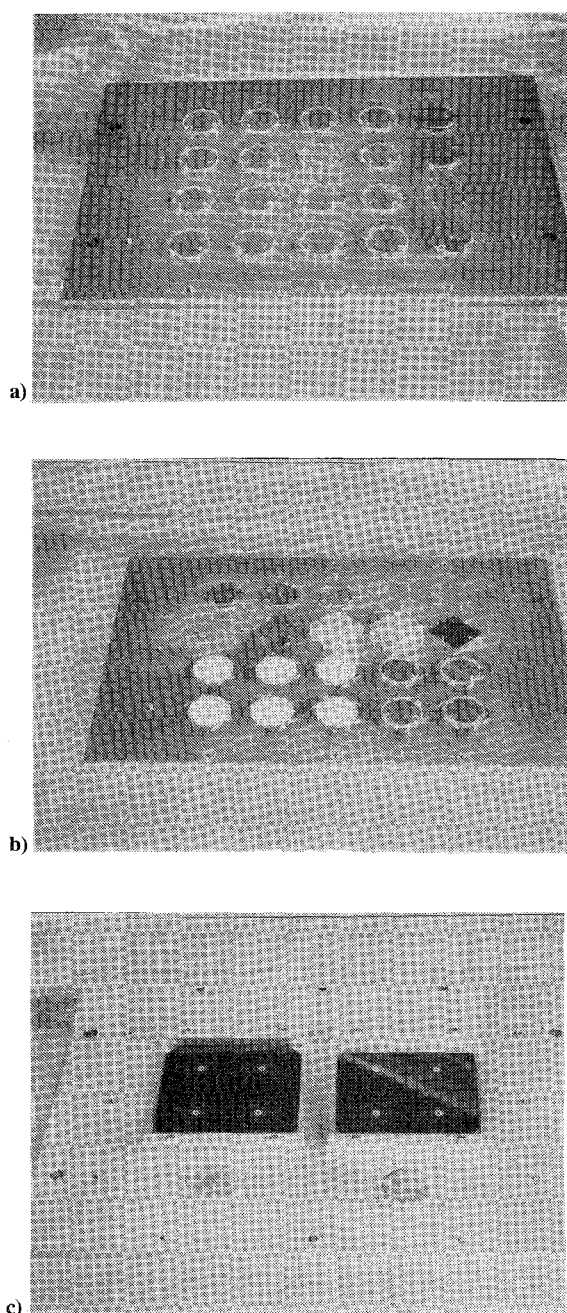


**Fig. 1** Sample trays for thruster exhaust contamination: a) tray 1, b) tray 2, and c) tray 3.

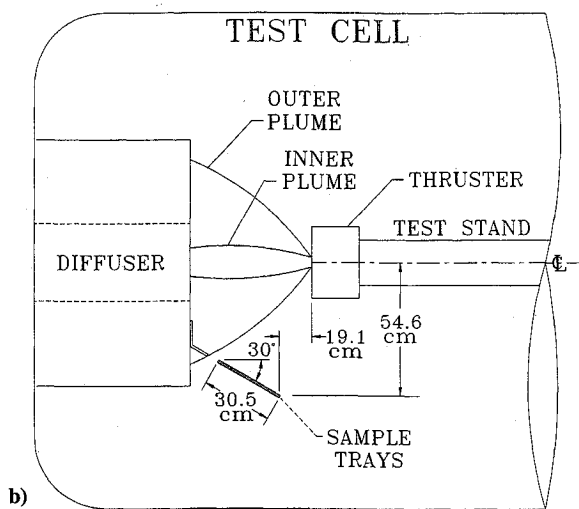
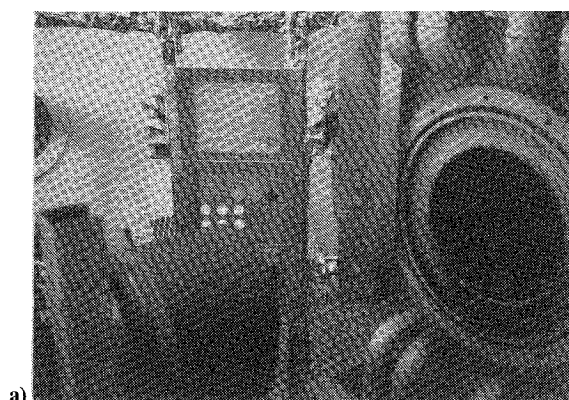


Fig. 2 Configuration of sample trays with respect to thruster: a) photograph of facility and b) top-view drawing of test cell.

(a top-view drawing of the test cell), the trays were mounted near the diffuser at an angle of approximately 30 deg to the centerline of the thruster. The diffuser, pumped by a gaseous-nitrogen ejection system, is used to expel the thruster exhaust from the test cell. Because the diameter of the plume at the front surface of the diffuser is larger than the diameter of the diffuser inlet, and because the diffuser surfaces are painted, a stainless-steel shield was placed between the diffuser and the sample trays in order to prevent paint particles and debris from being blown back onto the sample trays. The trays were mounted in an attempt to provide the maximum arrival of combustion by-products while minimizing the thermal load from the plume. Since the chamber is typically at a rough vacuum pressure during thruster operation, it was determined that the trays needed to be as close as possible to the outer edge of the plume to provide sufficient arrival of contamination in the absence of molecular flow. During the three thruster firing sequences, the test-cell pressure ranged from  $1.3 \times 10^3$  to  $5.3 \times 10^3$  Pa. The disadvantages of this test arrangement were that the background pressure was many orders of magnitude higher than that on orbit and that the samples were situated much closer to the plume than would occur for Space Station–Space Shuttle operations. Two free-standing thermocouples were installed at either end of tray 2 in order to provide an estimate of the temperature distribution across the surface of the sample trays. Thruster firing profiles show temperatures ranging from 93 to 260°C for the leading edge (away from diffuser) thermocouple and temperatures ranging from 177 to 427°C for the trailing edge (near diffuser) thermocouple. Although these temperatures are not representative of the samples themselves, they do give an indication of the temperatures of the environment. Because the samples were located so close to the plume, the temperatures were probably much higher than those that would be experienced for Space Station–Space Shuttle operations.

Between thruster exposures, the cell was purged to atmospheric pressure with nitrogen to allow suited personnel to enter and remove samples. The samples were placed in containers and sealed

in two nitrogen-purged bags. Upon removal from the cell, the samples were sealed in a third nitrogen-purged bag for transportation back to NASA Lewis Research Center. Samples were stored in these purged bags in a desiccator. The purged bags were not opened to atmosphere until immediately prior to exposure to the simulated LEO environments.

### Simulated LEO Environmental Exposures

#### Exposure to a Rough Vacuum Environment

A fused silica and a Z-93-P sample that had been exposed in the PRCS thruster facility for 61.2-s thruster-on time were placed in a vacuum desiccator and pumped to a pressure of approximately 4 Pa. Samples were kept in this environment for 120 h to determine the effects of exposure to vacuum on their optical properties.

#### Vacuum-Ultraviolet Radiation Exposure

Samples that had been previously exposed to a total of 91.8 s of PRCS thruster-on time were exposed to vacuum ultraviolet (VUV) radiation. These samples included chromic-acid-anodized aluminum, HEDB-anodized aluminum, Z-93-P, and two fused silica slides, including one that was coated with approximately 1200 Å of silicone fluid. The VUV exposure facility contains three water-cooled copper compartments each equipped with a 30-W deuterium lamp with a magnesium fluoride window. These compartments are located inside a cryopumped high-vacuum system bell jar, which operates at a pressure of approximately  $7 \times 10^{-4}$  Pa. Samples are placed on the floors of these compartments. The lamps provide VUV radiation predominantly in the wavelength range between 115 and 200 nm. The fused silica and Z-93-P samples received 312 equivalent sun hours (ESH) of VUV with an acceleration of 2.6 VUV suns, and the anodized aluminum samples received 276 ESH of VUV with an acceleration of 2.3 VUV suns, where the number of VUV suns refers to the ratio of the intensity of the test lamp to that of the sun at AM0 in the same wavelength range (115 to 200 nm). Prior to use, VUV lamps were calibrated with a photomultiplier tube (PMT) with a narrow-bandpass filter at 182 nm in air. The PMT was calibrated with a lamp calibrated by the National Institute of Standards and Technology (NIST). Because it was assumed that the NIST-calibrated lamp and the test lamps had the same spectral irradiance curve shape, relative irradiance values of the NIST-calibrated lamp between 115 and 200 nm were multiplied by the appropriate factor based on the measurement at 182 nm to obtain irradiance curves for the test lamps. The area under each irradiance curve was calculated to obtain the intensity between 115 and 200 nm. No long-term intensity monitoring was used.

#### Exposure to Atomic Oxygen and Vacuum-Ultraviolet Radiation

Thruster-exhaust-contaminated samples of Z-93-P and fused silica, including one fused silica sample which was also silicone-contaminated, were exposed to combined atomic oxygen (AO) and VUV radiation. Reference 12 describes the facility in detail. It uses an electron cyclotron resonance (ECR) plasma source to provide a low-energy (approximately 0.04 eV) directed AO beam. The base vacuum system pressure during AO exposure is approximately 0.08 Pa. Deuterium lamps of the same type used in the VUV facility were used to provide VUV radiation, and calibration was performed in the same manner. The effective AO flux and fluence were measured by the mass loss of Kapton®. The effective fluence ranged from  $1.3 \times 10^{21}$  to  $2.5 \times 10^{21}$  atoms/cm<sup>2</sup> at effective flux levels of  $2.7 \times 10^{15}$  to  $5.1 \times 10^{15}$  atoms/cm<sup>2</sup> · s. The VUV exposure consisted of 100 to 230 ESH at an intensity of 0.8 to 1.7 VUV suns. The AO and VUV radiation were not properly balanced to represent the actual space environment. The simulated environment was deficient in VUV exposure in comparison with the environment to which these materials would be exposed in space. The fused silica samples were exposed to an unknown level of additional VUV radiation from the AO source, expected to be predominantly at 130 nm because of their position with respect to the AO beam. The Z-93-P sample was shielded from this additional VUV radiation. The  $\alpha_s$  of Z-93-P was characterized in situ. Samples were also characterized for  $\alpha_s$  ex situ.

### Vacuum Thermal Cycling and Vacuum Ultraviolet Radiation Exposure

Following the thruster exposures, one of the solar cells was exposed to a total of 300 vacuum thermal cycles including approximately 300 ESH of VUV. Deuterium lamps were also used in this facility, and calibration was done as previously described. The temperature range for thermal cycling was between +80 and -80°C, and the VUV intensity was approximately 5 suns between 115 and 200 nm. The vacuum-system pressure was on the order of  $1 \times 10^{-4}$  Pa during this exposure. Reference 13 describes this facility in detail.

## Results and Discussion

### Characterization of Thruster-Exhaust Contamination

The contaminants present on a stainless-steel witness coupon exposed to 91.8 s of total thruster firing time were characterized by  $\mu$ -FTIR. The spectrum of this sample is shown in Fig. 3. This analysis indicated the presence of  $\text{NH}_3^+$  and  $\text{NO}_3^-$ , most likely indicating the presence of monomethylhydrazine nitrate (MMHN), which can be written as  $\text{CH}_3\text{NHNH}_3^+\text{NO}_3^-$ . The methyl ( $\text{CH}_3$ ) peak is known to be obscured by  $\text{NH}_3^+$ . MMHN is suspected to be the most significant contaminant from monomethylhydrazine-nitrogen tetroxide bipropellant thrusters. It has been found to be present on the walls of thruster facilities.<sup>1,2</sup> The shape of the infrared spectrum shown in Fig. 3 is similar to spectra obtained in previous studies of this type.<sup>1,2</sup>

Figure 4 shows the mass gain of stainless-steel witness coupons due to accumulation of contaminants from exposure in the thruster facility during pulsed firing operations. Data points for all witness coupons and estimated errors are shown. One witness sample was installed on the sample tray during the test setup, but was removed just before the thruster firings began. The objective of this procedure was to determine whether the environment in the test chamber would induce mass gain. Another sample was used as a control and was weighed with the other samples, but was not otherwise handled. Mass gains of both of these samples are shown at 0 s. The mass gain of the minimally handled control sample, which showed the larger gain, was considered to be the error in the mass measurements and was used in the calculation of the error bars for all data points. These data show that accumulation of contaminants is proportional to thruster firing time.

The amount of molecular deposition on Space Station surfaces provided by Space Shuttle thruster plumes during proximity operations is required not to exceed  $1 \times 10^{-6}$  g/cm<sup>2</sup> in a year of nominal operations based on an assessment of the external induced contam-

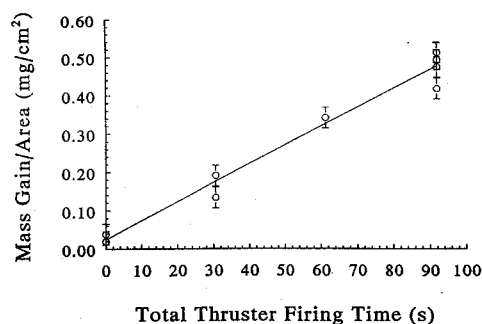


Fig. 3 Micro-FTIR spectrum of contaminants analyzed on stainless-steel sample.

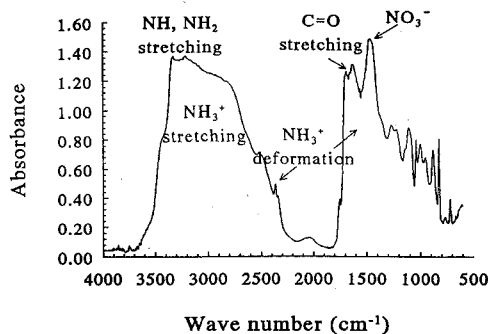


Fig. 4 Mass gain of thruster-exposed stainless-steel samples.

Table 2 Effects of thruster contaminants on optical properties

Sample type	Tray no.	Thruster on time, s	Optical properties			
			Preexposure		Postexposure	
			$\alpha_s$	$\epsilon_n$	$\alpha_s$	$\epsilon_n$
Fused silica	1	30.6	-0.003	—	0.078	—
Fused silica	1	61.2	-0.003	—	0.058	—
Fused silica with silicone oil	1	91.8	0.002	—	0.045	—
Chromic-acid-anodized Al	2	91.8	0.493	-743	0.516	0.798
Sulfuric-acid-anodized Al	2	91.8	0.461	0.863	0.490	0.884
HEDB-anodized Al	2	91.8	0.857	0.859	0.855	0.866
Z-93-P	2	61.2	0.097	—	0.122	—
Z-93-P	2	61.2	0.101	—	0.183	—
Z-93-P	2	61.2	—	0.917	—	0.908
Z-93-P	2	91.8	—	0.916	—	0.910
Z-93-P	2	91.8	0.102	0.915	0.135	0.910
Z-93-P	2	91.8	0.105	0.914	0.162	0.908

ination environment.<sup>14</sup> Furthermore, results of the Shuttle Plume Impingement Experiment implied that the mass of permanent contamination produced by the PRCS engine firings would be much less than that calculated in earlier assessments.<sup>6</sup> The coupons exposed in these experiments gained mass on the order of  $10^{-4}$  g/cm<sup>2</sup>. Clearly these coupons received a much greater amount of contamination than surfaces in space would receive over the lifetime of the Space Station. Therefore, the changes in optical properties due to deposition of such a large amount of contamination are expected to be worse than would actually occur in space.

### Effects of Deposited Contaminants on Optical Properties of Samples

Table 2 shows  $\alpha_s$  and  $\epsilon_n$  values for samples before and after thruster exposure for fused silica slides, anodized aluminum samples, and Z-93-P samples. Samples with initially low  $\alpha_s$  showed significant increases due to the contamination. The HEDB-anodized aluminum sample, which had the highest initial  $\alpha_s$ , showed a negligible increase. It is expected that  $\epsilon_n$  of the contaminant is between the  $\epsilon_n$  of the anodized aluminum specimens (0.743 to 0.863) and the  $\epsilon_n$  of Z-93-P (0.914 to 0.917), because the anodized aluminum samples show increases in  $\epsilon_n$ , whereas the Z-93-P samples show decreases in  $\epsilon_n$ . In view of the scatter in the data, there does not appear to be a significant correlation between  $\alpha_s$  increase and thruster exposure time.

### Subsequent Simulated LEO Exposure of Contaminated Samples

#### Exposure to Rough Vacuum

A sample of fused silica and a sample of Z-93-P were exposed in a rough vacuum of approximately 4 Pa for 120 h. The fused silica sample showed an increase in solar absorptance of 0.006, from 0.025 before exposure to 0.031 after exposure. Because the error in repeatability of the spectrophotometer is considered to be approximately  $\pm 0.005$ , this change is within the error of the instrument. The Z-93-P sample showed a reduction in  $\alpha_s$  of 0.007, from 0.133 before exposure to 0.126 after exposure, again within error of instrument repeatability. The purpose of this experiment was to determine whether dehydration of the deposited thruster contaminants would result in restoration of original optical properties of the sample and thus removal of the contaminants. These data show that dehydration of the contaminant did not cause it to completely volatilize from the sample surface. Therefore, any significant changes in optical properties of samples exposed to simulated LEO environments were not due simply to exposure to vacuum.

#### Exposure to VUV Radiation

Table 3 shows the optical properties of samples exposed to between 276 and 312 ESH of VUV radiation. The samples had previously been exposed to 91.8 s of total thruster firing time. For solar-cell materials, which would be sun-facing, the 312-ESH exposure represented only approximately 18 days in space. The anodized

aluminum samples were exposed to 276 ESH, which is equivalent to approximately 15 days in space. For the Z-93-P coating, which would not be sun-facing, but could receive small amounts of sun exposure due to small errors in positioning of the radiator, exposure to 312 ESH represented approximately 330 days in space. The initially low-solar-absorptance materials, fused silica and Z-93-P, displayed increases in  $\alpha_s$  that are outside of the error of the spectrophotometer. Both the Z-93-P sample and the fused silica with silicone oil showed increases in  $\alpha_s$  of 0.016 when measured in air. This may be indicative of darkening of the contaminants on the surfaces. In space, a surface that became contaminated with thruster contaminants and/or with silicone contaminants may experience degradation in  $\alpha_s$  with solar ultraviolet radiation exposure. Note that the  $\epsilon_n$  values of Z-93-P and HEDB-anodized aluminum changed only slightly with this exposure, whereas the chromic-acid-anodized aluminum showed a measurable decrease in  $\epsilon_n$ . The reason for the change in this sample is not known.

#### Exposure to Atomic Oxygen and VUV Radiation

Table 4 shows the results of exposure of samples of fused silica, fused silica with silicone oil, and Z-93-P, all of which had previously been contaminated by thruster exhaust, to AO combined with VUV radiation. The levels of AO and VUV exposure are shown. Also shown is the ratio of AO fluence to VUV equivalent sun hours experienced in the facility divided by the value of the same ratio required by the Space Station for solar cells (represented by fused silica) and radiator surfaces (represented by Z-93-P). Photovoltaic-power-system radiator surfaces on the Space Station, including the Z-93-P coating, are required to survive exposure to approximately  $1.7 \times 10^{22}$  atoms/cm<sup>2</sup> and 5160 h of solar ultraviolet radiation over a mission life of 15 years.<sup>15</sup> Solar-facing solar-array surfaces on the Space Station are required to survive an AO fluence of approximately  $4.3 \times 10^{22}$  atoms/cm<sup>2</sup> and up to approximately 97,500 h of solar ultraviolet radiation in 15 years.<sup>16,17</sup> The ratio of AO/VUV<sub>Test</sub> to AO/VUV<sub>SS</sub> indicates the imbalance in the ratio of AO fluence to VUV equivalent sun hours experienced by the test coupons as compared to what is expected on the Space Station. Note that the AO dose in this test exceeded the VUV dose for comparison with the Space Station environment. The fused silica materials experienced

more of an excess of AO than the Z-93-P, as indicated by the fact that the ratio was much greater for the fused silica samples.

Values of  $\alpha_s$  for all of the fused silica samples decreased, indicating that AO reacted with the contaminants on the surface and oxidized them, thus either removing or bleaching them. The AO-VUV exposure did significantly reduce  $\alpha_s$ , although it did not restore the original  $\alpha_s$  values measured prior to thruster-exhaust contamination. One possible conclusion that can be drawn from these data for solar cells that contain cover glass is that contamination may not severely compromise performance as long as the cells are in an atomic-oxygen environment. However, caution must be used in interpreting these results with respect to the Space Station, because the test environment contained a much greater AO dose in comparison with VUV than would occur for Space Station surfaces.

The in situ measurements of Z-93-P before and after AO-VUV exposure showed an increase in  $\alpha_s$  of 0.03, whereas the ex situ measurements showed a decrease of 0.06. Exposure of uncontaminated Z-93-P samples in the same facility have shown significant  $\alpha_s$  degradation due to color-center formation, which was reversible upon exposure to air.<sup>15</sup> Therefore, it is expected that the degradation observed in this test is dominated by color-center formation in the Z-93-P coating, although VUV darkening of surface contamination may contribute slightly to this degradation. Because the sample was removed from vacuum, and VUV-induced color centers were likely eliminated, the reduction in  $\alpha_s$  for Z-93-P samples likely indicates bleaching and/or removal of contamination similar to that for the fused silica samples.

Note that the pre-exposure in situ and ex situ  $\alpha_s$  values are different. There are two contributors to this difference. First, exposure of a Z-93-P sample in a rough vacuum caused a 0.007 reduction in  $\alpha_s$ . Second, it is likely that there is a difference in accuracy between the two instruments used to obtain in situ and ex situ  $\alpha_s$  values. Both instruments have good repeatability, and, because the purpose of these investigations was to determine changes in  $\alpha_s$  due to exposure to the AO-VUV environment, attempts were not made at this time to correlate the two instruments.

#### Solar-Cell Performance

Figure 5 shows changes in solar-cell efficiency as a function of the various treatments for two cells labeled SC-1 and SC-3. The efficiency is the ratio of the measured power output of the cell to the power input from the solar simulator. Error bars are included. Note that exposure to Al<sub>2</sub>O<sub>3</sub> and the thruster contaminants resulted in some performance degradation. Exposure to the first 150 VUV-thermal cycles indicated continued degradation. After exposure to another 150 cycles, for a total of 300 VUV-thermal cycles, a slight improvement was observed. However, the measured cell efficiencies after VUV-thermal cycling may be within error of the measured cell efficiency prior to this exposure. Therefore, the indicated changes due to VUV-thermal cycling may not be significant. One may conclude that exposure of solar cells to an environment containing temperature cycling and solar ultraviolet radiation would probably not improve cell efficiency, but may not further the degradation. Because of the facility limitations, only one cell was able to be tested

**Table 3 VUV radiation effects on optical properties of contaminated samples**

Sample type	Tray no.	ESH VUV @ no. of suns	Optical properties			
			Before VUV		After VUV	
			$\alpha_s$	$\epsilon_n$	$\alpha_s$	$\epsilon_n$
Fused silica	1	312@2.6	0.027	—	0.038	—
Fused silica with silicone oil	1	312@2.6	0.020	—	0.036	—
Z-93-P	2	312@2.6	0.141	0.910	0.157	0.912
Chromic-acid-anodized Al	2	276@2.3	0.550	0.798	0.558	0.786
HEDB-anodized Al	2	276@2.3	0.856	0.866	0.848	0.867

**Table 4 AO/VUV exposure effects on solar absorptance of contaminated samples**

Sample type	Thruster firing time, s	Effective AO fluence, at./cm <sup>2</sup> , @ flux, at./cm <sup>2</sup> s	ESH VUV @ no. of suns	(AO/VUV) <sub>Test</sub> (AO/VUV) <sub>SS</sub>	Solar absorptance	
					Before exposure	After exposure
Fused silica	30.6	$2.6 \times 10^{21}$ @ $5.1 \times 10^{15}$	105 @0.79	49	0.078	0.008
Fused silica/silicone oil	91.8	$2.0 \times 10^{21}$ @ $4.1 \times 10^{15}$	147 @1.1	27	0.045	0.021
Fused silica	61.2	$2.0 \times 10^{21}$ @ $4.1 \times 10^{15}$	147 @1.1	27	0.058	0.015
Z-93-P in situ	61.2	$6.8 \times 10^{20}$ @ $3.0 \times 10^{15}$	103 @1.7	3.1	0.167	0.196
Z-93-P ex situ	61.2	$1.3 \times 10^{21}$ @ $2.7 \times 10^{15}$	226 @1.7	2.7	0.183	0.122

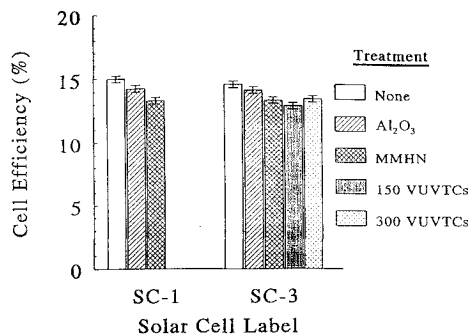


Fig. 5 Combined contamination and simulated LEO environmental effects on solar-cell efficiency.

in this manner. Additional tests would allow statistical correlations to be made. In view of the effect of AO-VUV exposure on the fused silica samples, which was to decrease  $\alpha_s$ , it is likely that an environment containing AO would restore some of the efficiency of the contaminated cells.

### Conclusions

Exposure of fused silica slides and thermal control surfaces to exhaust from a Space Shuttle-type thruster in a rough vacuum facility resulted in significant  $\alpha_s$  increases in tests where the pressure, temperature, and amount of deposited contaminants well exceeded those expected for Space Station surfaces. This performance loss was reversed to a great extent by subsequent exposure to an environment containing an excess of AO over the VUV radiation expected for Space Station surfaces. In situ measurements indicated an increase in  $\alpha_s$  for thruster-exhaust-contaminated Z-93-P exposed to AO and VUV, whereas ex situ measurements showed a decrease in  $\alpha_s$ . It is likely that this is predominantly due to VUV radiation effects on the Z-93-P material, which are reversible upon exposure to air. The VUV radiation environment alone caused some degradation of previously contaminated anodized aluminum, Z-93-P, and fused silica. This indicates that solar ultraviolet radiation alone can react with deposited thruster contaminants resulting in a darkened film.

Aluminum oxide and thruster-exhaust contamination reduced the efficiency of solar cells. Subsequent thermal cycling combined with VUV radiation exposure did not result in continued degradation. Also, results from the AO-VUV exposure of fused silica indicate that AO exposure of contaminated cells would likely result in some restoration of cell efficiency due to bleaching or removal of contaminants.

### Acknowledgments

The authors would like to acknowledge the technical support of the following: Sharon K. Rutledge, Kim K. de Groh, and Marla E. Perez-Davis of the Electro-Physics Branch at NASA Lewis Research Center; Bryan K. Smith and Marian C. Felder of the Solar Array Branch at NASA Lewis Research Center; Robert Cort of NASA Johnson Space Center/White Sands Test Facility; Gerald F. Winans of Lockheed Engineering & Sciences CO., supporting White Sands Test Facility; Pilar C. Herrera-Fierro of Case Western Reserve University supporting the NASA LeRC Surface Science Branch; Daniel A. Scheiman of NYMA, Inc., supporting the NASA LeRC Polymers Branch; Tim McCollum and Ed Sechkar of Cleveland State University; personnel from Illinois Institute of Technology Research Institute; and personnel from the Space Station Division of McDonnell Douglas Aerospace, especially Cherie A. Jones and Huong G. Le.

### References

- <sup>1</sup>Etheridge, F. G., and Boudreaux, R. A., "Attitude-Control Rocket Exhaust Plume Effect on Spacecraft Functional Surfaces," *Journal of Spacecraft and Rockets*, Vol. 7, No. 1, 1970, pp. 44-48.
- <sup>2</sup>Takimoto, H. H., and Denault, G. D., "Rocket Plume ( $N_2O_4/MMH$ ) Impingement on Aluminum Surface," *Journal of Spacecraft and Rockets*, Vol. 7, No. 11, 1970, pp. 1372-1374.
- <sup>3</sup>Jack, J. R., Spisz, E. W., and Cassidy, J. F., "The Effect of Rocket Plume Contamination on the Optical Properties of Transmitting and Reflecting Materials," AIAA Paper 72-56, Jan. 1972.
- <sup>4</sup>Bowman, R. L., Spisz, E. W., and Jack, J. R., "Effect of Contamination on the Optical Properties of Transmitting and Reflecting Materials Exposed to a  $MMH/N_2O_4$  Rocket Exhaust," NASA TM X-68204, Apr. 1973.
- <sup>5</sup>Liu, C., and Glassford, A. P. M., "Contamination Effect of  $MMH/N_2O_4$  Rocket Plume Product Deposit," *Journal of Spacecraft and Rockets*, Vol. 18, No. 4, 1981, pp. 306-311.
- <sup>6</sup>Koontz, S., Ehlers, H., Pedley, M., Hakes, C., and Cross, J., "Shuttle Primary Reaction Control System (PRCS) Engine Exhaust Plume Contamination Effects: The Shuttle Plume Impingement Experiment (SPIE), STS-52," AIAA Paper 93-0618, Jan. 1993.
- <sup>7</sup>Tribble, A. C., "Low Earth Orbit Plasma Effects on Spacecraft," AIAA Paper 93-0614, Jan. 1993.
- <sup>8</sup>Banks, B. A., Dever, J. A., Gebauer, L., and Hill, C. M., "Atomic Oxygen Interactions with FEP Teflon and Silicones on LDEF," *LDEF-69 Months in Space*, NASA CP 3134, Pt. 2, June 1991, pp. 801-815.
- <sup>9</sup>Stewart, T. B., Arnold, G. S., Hall, D. F., and Marten, H. D., "Photolysis of Spacecraft Contaminants," The Aerospace Corp., Rept. SD-TR-89-45, El Segundo, CA, July 1989.
- <sup>10</sup>Stewart, T. B., Arnold, G. S., Hall, D. F., Marvin, D. C., Hwang, W. C., Young Owl, R. C., and Marten, H. D., "Photochemical Spacecraft Self-Contamination: Laboratory Results and Systems Impacts," The Aerospace Corp., Rept. TOR-0090 (5470-01)-3, El Segundo, CA, July 1990.
- <sup>11</sup>Seiber, B. L., Bertrand, W. T., and Wood, B. E., "Contamination Effects of Satellite Material Outgassing Products on Thermal Surfaces and Solar Cells," Arnold Engineering Development Center, Rept. AEDC-TR-90-27, Arnold AFB, TN, Dec. 1990.
- <sup>12</sup>Stidham, C. R., Stueber, T. J., Banks, B. A., Dever, J. A., Rutledge, S. K., and Bruckner, E. J., "Low Earth Orbital Atomic Oxygen Environmental Simulation Facility for Space Materials Evaluation," *Proceedings of the 38th International SAMPE Symposium and Exhibition, Advanced Materials: Performance Through Technology Insertion*, edited by V. Bailey, G. C. Janicki, and T. Haulik, Science of Advanced Materials and Process Engineering Series, Vol. 38, Book 1, 1993, Society for the Advancement of Material and Process Engineering, Covina, CA, 1993, pp. 649-663.
- <sup>13</sup>Dever, J. A., de Groh, K. K., Stidham, C. R., Stueber, T. J., Dever, T. M., Rodriguez, E., and Terlep, J., "Simulation of the Synergistic Low Earth Orbit Effects of Vacuum Thermal Cycling, Vacuum UV Radiation and Atomic Oxygen," *Terrestrial Test for Space Success, Proceedings of the 17th Space Simulation Conference*, NASA CP 3181, Greenbelt, MD, 1992, pp. 19-36.
- <sup>14</sup>Leger, L., Ehlers, H., Hakes, C., Theall, J., and Soares, C., "External Induced Contamination Environment Assessment for Space Station Freedom," AIAA Paper 93-0617, Jan. 1993.
- <sup>15</sup>Dever, J. A., Rutledge, S. K., Bruckner, E. J., Stidham, C. R., Stueber, T. J., and Booth, R. E., "The Effects of Simulated Low Earth Orbit Environments on Spacecraft Thermal Control Coatings," *Advanced Materials: Performance Through Technology Insertion*, edited by V. Bailey, G. C. Janicki, and T. Haulik, Science of Advanced Materials and Process Engineering Series, Vol. 38, Book 1, Society for the Advancement of Material and Process Engineering, Covina, CA, 1993, pp. 694-706.
- <sup>16</sup>Stidham, C. R., Stueber, T. J., Banks, B. A., Dever, J. A., and Rutledge, S. K., "Low Earth Orbital Atomic Oxygen Environmental Simulation Facility for Space Materials Evaluation," *Advanced Materials: Performance Through Technology Insertion*, edited by V. Bailey, G. C. Janicki, and T. Haulik, Science of Advanced Materials and Process Engineering Series, Society for the Advancement of Material and Process Engineering, Covina, CA, 1993, pp. 649-663.
- <sup>17</sup>Jones, C. A., private communication, McDonnell Douglas Aeronautics, March 1994.